DESIGN, CONSTRUCTION AND EVALUATION OF AN ULTRASONIC GAS ATOMIZER FOR PRODUCTION OF ALUMINIUM MATRIX COMPOSITES BY MEANS OF OSPREY PROCESS

D. Atehortua[1], J. Gonzalez[1], H. Sanchez[1**], W. Barona[1], J. Portocarrero[2]*

- ✓ Este artículo forma parte del "Volumen Suplemento" **S1** de *la Revista Latinoamericana de Metalurgia y Materiales* (*RLMM*). Los suplementos de la RLMM son números especiales de la revista dedicados a publicar memorias de congresos.
- ✓ Este suplemento constituye las memorias del congreso "*X Iberoamericano de Metalurgia y Materiales (X IBEROMET)*" celebrado en Cartagena, Colombia, del 13 al 17 de Octubre de 2008.
- ✓ La selección y arbitraje de los trabajos que aparecen en este suplemento fue responsabilidad del Comité Organizador del *X IBEROMET*, quien nombró una comisión *ad-hoc* para este fin (véase editorial de este suplemento).
- ✓ La *RLMM* no sometió estos artículos al proceso regular de arbitraje que utiliza la revista para los números regulares de la misma.
- ✓ Se recomendó el uso de las "Instrucciones para Autores" establecidas por la *RLMM* para la elaboración de los artículos. No obstante, la revisión principal del formato de los artículos que aparecen en este suplemento fue responsabilidad del Comité Organizador del *X IBEROMET*.

Suplemento de la Revista Latinoamericana de Metalurgia y Materiales 2009; **S1** (4): 1403-1410

DESIGN, CONSTRUCTION AND EVALUATION OF AN ULTRASONIC GAS ATOMIZER FOR PRODUCTION OF ALUMINIUM MATRIX COMPOSITES BY MEANS OF OSPREY PROCESS

D. Atehortua[1], J. Gonzalez[1], H. Sanchez[1**], W. Barona[1], J. Portocarrero[2]*

1. University of Valle, Material Engineering School.
2. Militar Aviation School, Cali, Colombia.

** E-mail: daferalo@hotmail.com, hsestepa@univalle.edu.co*

Trabajos presentados en el X CONGRESO IBEROAMERICANO DE METALURGIA Y MATERIALES IBEROMET
Cartagena de Indias (Colombia), 13 al 17 de Octubre de 2008

Selección de trabajos a cargo de los organizadores del evento

Publicado On-Line el 29-Jul-2009
Disponible en: *www.polimeros.labb.usb.ve/RLMM/home.html*

Abstract

In this work a confined-type Ultrasonic Gas Atomizer was designed for the *Osprey* process developed at the University of Valle. An annular ring-shaped nozzle was selected for the atomizer, so that it could be possible to achieve a maximum gas mass flux rate $\dot{G}$, which is desirable to make the liquid metal disintegration process easier. In order to design the atomizer, some values used in geometrical features of different atomizers of this type were selected. Then, the resulting parameters of the gas behavior, such as gas mass flux rates $\dot{G}$, were theoretically calculated according to fluid mechanic models, for a specific atomization pressure range P_o, and for an inert-to-metal gas atomization media, like N_2. Then ALGOR® computer program was used to evaluate the mechanical behavior of the designed atomizer within atomization pressure range at which it was expected to work. After the atomizer was constructed, it was found that the protrusion distance of the delivery tube *h* at which the maximum aspirating pressure at the exit of the liquid metal is achieved is 8 mm. Then, the non-ideal gas equations, and the N_2 pipe discharge curves at some atomization pressures were used in order to find the actual gas mass flux rates. The obtained results showed that they were 81% that of the theoretically calculated ones, partially because of the effect known as "Vena Contracta". In addition to that, atomization tests with water and wax were carried out, measuring the water mass flux rate $\dot{M}$. Finally, preliminary atomization tests with aluminum were carried out. 40 and 80 μm diameter aluminum powders were obtained at a manometric atomization pressure of 0,69 MPa.

Keywords: *Ultrasonic Gas Atomization, Aspiration Pressure, Protrusion Distance, Aluminum Atomization.*

Resumen

En este trabajo se diseño un atomizador de gas ultrasónico de tipo confinado para el proceso *Osprey* desarrollado en la Universidad del Valle. Además, para el atomizador se seleccionó una boquilla en forma de anillo, de modo que fuera posible lograr un máximo flujo másico del gas $\dot{G}$, lo cual es deseable para facilitar el proceso de desintegración del metal. Para diseñar el atomizador, se seleccionaron algunos valores usados en las dimensiones de diferentes atomizadores de este tipo. Luego, los parámetros resultantes del comportamiento del gas, como los flujos másicos $\dot{G}$, fueron calculados teóricamente de acuerdo a ciertos modelos de mecánica de fluidos, para un rango de presiones P_o específico, y para un medio de atomización inerte al metal, como el N_2. Luego se utilizó el programa de computador ALGOR® para evaluar el comportamiento mecánico del diseño dentro del rango de presiones de atomización en el cual se espera que trabaje el atomizador. Después de construido, se encontró que la distancia de protrusión *h* del bajante a la cual se logra la máxima presión de aspiración a la salida del metal líquido es 8 mm. Luego, se utilizaron las ecuaciones de los gases reales y las curvas de descarga de las pipas de N_2 a determinada presión de atomización para hallar los flujos másicos reales del gas, encontrando que son en promedio un 81% de los calculados teóricamente, en parte debido al efecto conocido como "Vena Contracta". Además, se realizaron pruebas de atomización con agua y con cera, midiendo el flujo másico de agua $\dot{M}$. Finalmente, se llevaron a cabo pruebas preliminares de atomización con aluminio, obteniendo polvos con un diámetro entre 40 y 80 μm a una presión manométrica de atomización de 0,69 MPa.

Palabras Claves*: Atomización con gas ultrasónica, Presión de aspiración, Distancia de protrusión, Atomización de aluminio.*

1. INTRODUCTION

Atomization is the most critical step in *Osprey* Process [1], since process success mainly depends on effective conversion of liquid metal into fine droplets, because the finer are the droplets, the better are material properties [2].

There are different types of atomization, but confined-type Ultrasonic Gas Atomization (USGA) is one of the most preferred techniques used in the *Osprey* Process [1]; its nozzle design include resonance cavities in order to produce a combined flow pattern between high pressure and interference, so that the gas speeds up quickly as it passes through the cavities, generating an ultrasonic shock wave sequence which is carried by the gas (see Figure 1).

In a confined-type atomizer, the bulk liquid metal is kept confined by the delivery tube, at the end of which the interaction with the atomization media happens [3]. Due to the high speed of the gas flow next to the exit of the delivery tube, an important feature of a confined-type atomizer is that under certain special conditions, it is possible to get an aspiration pressure zone at that point, which is able to control the liquid metal output rate; just the same, that configuration avoids wasting great quantities of kinetic energy of the gas **¡Error! No se encuentra el origen de la referencia.**].

In a confined-type USGA, the gas leaves the nozzle in a supersonic velocity regimen, which is said to be produced by the effect known as "Vena Contracta" [2] (see Figure 2); that effect consists in a growth of a boundary layer that reduces the effective area for gas flow. However, this effect is not well understood yet. Theoretically, the ultrasonic shock waves increase the atomizer global efficiency because they supply an extra energy that contributes to the bulk liquid metal disintegration process.

For the *Osprey* process, it is necessary that the atomized droplets achieve special requirements in regard to size distribution, mean mass diameter and their morphology, because those characteristics influence strongly the final microstructure of the material [2]. That is why confined-type USGA is useful for the process, because it allows exerting a close control over powder composition, cleanness, mean mass diameter d_m, size distribution and morphology. Generally speaking, the overall energy efficiency is very low, being on the order of 3% [2].

Although gas atomization is a frequent topic in the literature, it is not possible to find engineering data on the design and characterization of an atomizer for a given application, because atomizers are proprietary **¡Error! No se encuentra el origen de la referencia.**].

In this paper, a confined-type ultrasonic gas atomizer is designed, constructed and evaluated for being used in an *Osprey* process.

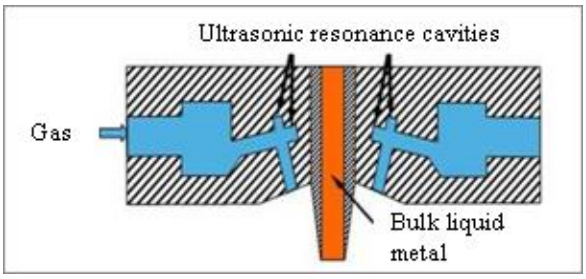


Figure 1. Diagram of the nozzle in a USGA.

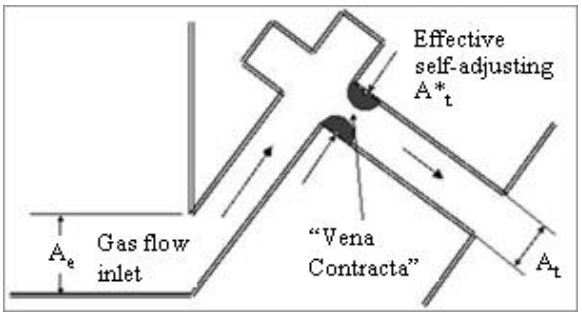


Figure 2. Schematic of resonance cavities and effective throat in a USGA nozzle (not to scale). Reduction in throat area, yielding and effective A^*_t, is shown (highly exaggerated).

2. ATOMIZER DESIGN

Normally, in spite of the fact that there are some one-phase fluid mechanic models that allow predicting, until some extent, the behavior of gas flowing through an atomizer, it is pretty difficult to predict accurately the behavior of the interaction gas - liquid metal even if advanced computational programs are used (i.e. CFD tools), so that designers cannot know easily *a priori* how to produce determined powder properties as a result of the atomization process; there are so many variables involved and their relationships are too complex. That is why designing a confined-type atomizer and getting the precise operational window is usually a matter of trial and error **¡Error! No se encuentra el origen de la referencia.**].

In order to design the atomizer, getting a particular

high range of gas mass flux rates $\dot{G}$ was considered as the main criteria, because the higher is $\dot{G}$, the lower is the produced mean mass diameter d_m, as it is predicted by the Lubanska´s model [5]:

$$d_m = KD\left[\frac{\nu_l}{\nu_g We}\left(1+\frac{\dot{M}}{\dot{G}}\right)\right]^{1/2} \quad (1)$$

Where D is the inner diameter of the delivery tube, $\dot{M}$ is the metal mass flux rate, ν_l and ν_g are kinematics viscosities of metal and gas respectively, K is a constant which depends on atomizer design and We is the Webber number.

Just the same, $\dot{G}$ depends mainly on atomization pressure p_o and atomizer geometry, according to the following equation, for a supersonic velocity regimen [2]:

$$\dot{G} = A_t\left[\gamma\rho_o p_o\left(\frac{2}{\gamma+1}\right)^{\frac{(\gamma+1)}{(\gamma-1)}}\right]^{1/2} \quad (2)$$

Where A_t is the total outlet area of the nozzle (in this case), γ and ρ_o are constant pressure and constant volume heat capacity relation, and gas density at p_o, respectively.

Taking different values for A_t and p_o, after three iterations the results of $\dot{G}$ shown in Table 1 were computed from selected atomizer geometry (see Table 2), which was chosen according to some values used in geometrical dimensions of different atomizers of this type [6].

Table 1. Calculation of gas mass flux rates $\dot{G}$ as function of atomization pressure p_o, according to equation (2).

P_o (MPa)*	T (K)	γ	ρ_o (Kg/m^3)	$\dot{G}$ (Kg/s)	$\dot{G}$ (Kg/min)
0,1	298	1,403	2,267	0,008	0,484
0,2	298	1,405	3,404	0,012	0,727
0,3	298	1,407	4,540	0,016	0,969
0,4	298	1,408	5,677	0,020	1,211
0,5	298	1,410	6,813	0,024	1,454
0,6	298	1,412	7,949	0,028	1,697
0,7	298	1,414	9,086	0,032	1,940
0,8	298	1,416	10,222	0,036	2,183
0,9	298	1,417	11,359	0,040	2,426
1,0	298	1,419	12,495	0,045	2,670
1,1	298	1,421	13,632	0,049	2,914
1,2	298	1,423	14,768	0,053	3,159
1,3	298	1,425	15,905	0,057	3,403
1,4	298	1,426	17,041	0,061	3,647
1,5	298	1,428	18,178	0,065	3,892

* Manometric pressure

Gas thermodynamic properties can be found elsewhere [7].

Table 2. Selected parameters for the atomizer design (see Figure 3).

Parameter	Symbol	Chosen Value
Delivery tube outter radius	R (mm)	5
Ring outter radius	r_g/R	1,11
Apex angle	Θ	22,5º
Tip angle of the delivery tube	α	22,5º
Delivery tube inner radius	r_n/R	0,3
Atomization gas		N_2
Atomization chamber pressure	P_m (atm)	1
Atomization chamber temperature	T_m (K)	298
Total gas inlet area of the nozzle	A_e (m^2)	3,46E-05
Total gas outlet area of the nozzle	A_t (m^2)	1,74E-05

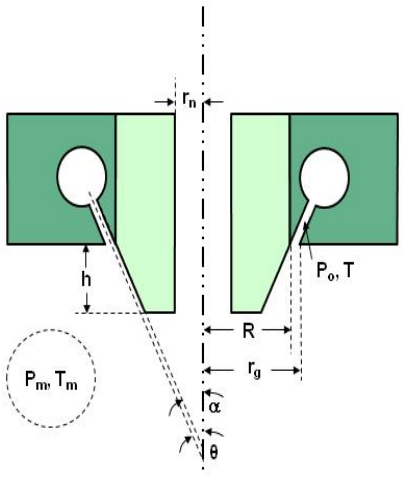


Figure 3. Diagram of a confined-type atomizer with an annular ring-shape nozzle, where the geometric features are shown (see Table 2).

2.1 Mechanical design

Once the atomization pressure range was known, ALGOR® was used in order to simulate the

mechanical behavior of the atomizer working at the maximum atomization pressure. A summary of the results can be seen in Figure 4. It could be noted that nor stresses nor misplacements are dangerous for the integrity of the atomizer, and mechanically speaking, the proposed design is well away from a failure. Selected material of the atomizer was a tempered 4340 AISI steel. More details of the analysis can be found in literature [1].

The resulting atomizer design is sketched in Figure 5, and its actual dimensions can be appreciated there.

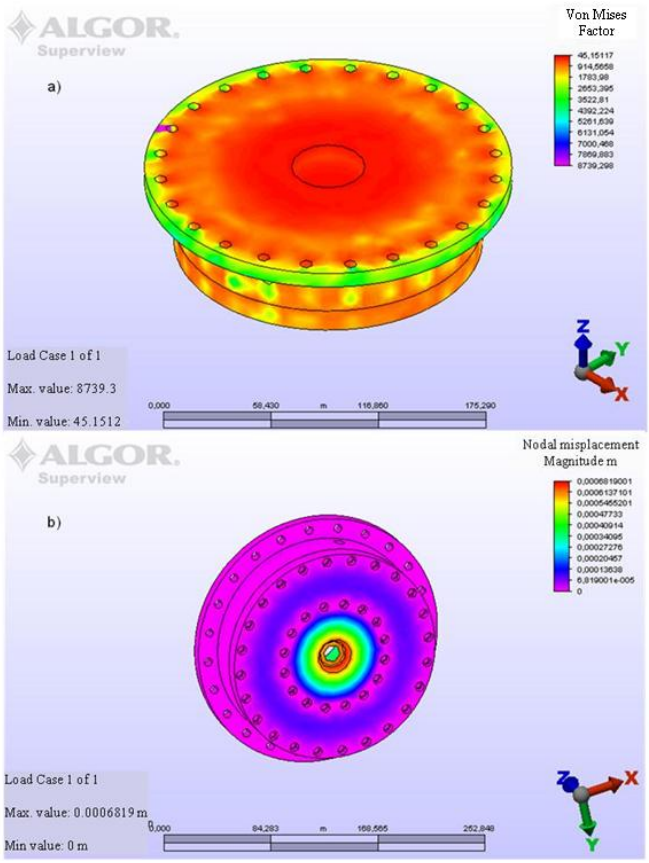


Figure 4. ALGOR Simulation test of the proposed atomizer design working at the expected maximum atomization pressure (1.5 MPa): a) Von Mises Factor, b) Nodal misplacement magnitude.

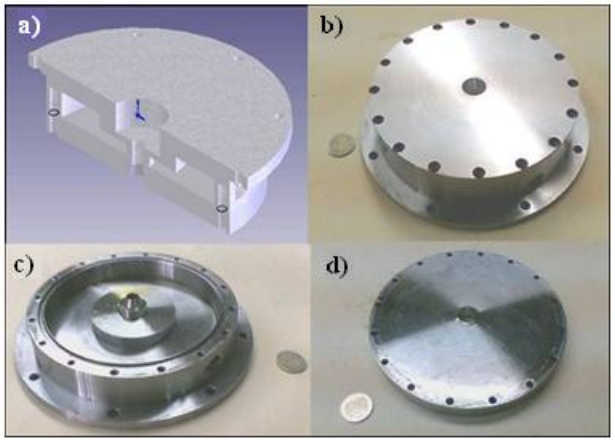


Figure 5. Resulting atomizer design for the *Osprey* process: a) a sketch of the design assembly, b) Picture showing the complete atomizer assembly, c) Picture showing the body of the atomizer, and d) Picture showing the bottom of the atomizer.

3. EXPERIMENTAL PROCEDURE

A general methodology for evaluating the behavior of an atomizer is described somewhere [1, 4, 8, 9], and it has been used in this work in order to evaluate this atomizer. It is explained as follows:

3.1 Determination of the protrusion distance of the delivery tube *h*

One important characteristic of the operation of the atomizer is that at the end of the liquid delivery tube a pressure zone is established, which mainly depends on protrusion distance of the delivery tube h and atomization pressure P_o. If the value of the pressure at that point is lower than the atomization chamber pressure, an aspiration pressure zone is created, which is desirable in order to exert a close control over the mass flux rate $\dot{M}$, avoiding the freeze-up of the metal inside the tube. Accordingly, it is necessary to determinate the conditions that allow getting an aspiration pressure zone.

Tests were carried out varying the protrusion distance of the delivery tube h and atomization pressure P_o simultaneously, while the rest of the parameters of the atomizer were kept constant (see Table 2). Gas pressure at the end of delivery tube was measured by means of a vacuum manometer as shown in Figure 6. The accuracy of pressure gauge was better than 0,002 MPa.

3.2 Measurements of gas mass flux rates $\dot{G}$

In order to measure $\dot{G}$, a series of pipe discharge curves were obtained from measuring pipe pressure

against time for two different atomization pressures. An ASHCROFT® digital manometer with 2000 psi of capacity and an accuracy of 1 psi was used for measuring pipe pressure. Also, pipe and jet temperature at the exit of the atomizer was measured with a thermocouple (accuracy better than 1 K). The experimental assembly was similar to the one shown in Figure 6.

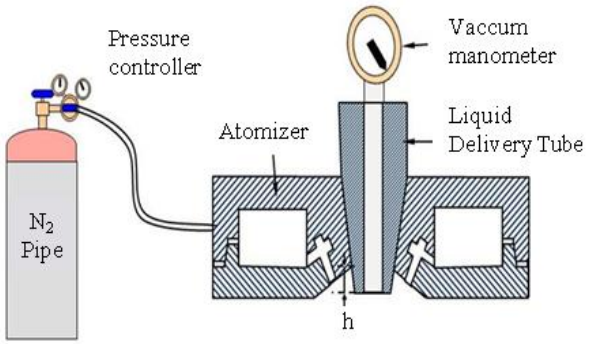


Figure 6. A sketch of the experimental assembly used for finding the ideal protrusion distance of the delivery tube *h*.

Then, Van der Waals and Redlich-Kwong non-ideal gas equations [10] were used for computing remained gas mass in the pipe which, plotted against time, allowed calculating $\dot{G}$, since it is equal to the slope of the curve.

3.3 Measurements of water mass flux rates $\dot{M}$

In order to simulate the behavior of the liquid aluminum flow during atomization process, atomization test with water were carried out at two different values of *h* within an atomization pressure range, measuring water mass flux rates $\dot{M}$ by means of plotting the height of the water column $\mathbf{h_m}$ against time, always taking 45 cm as the starting point. The experimental assembly is shown in Figure 7.

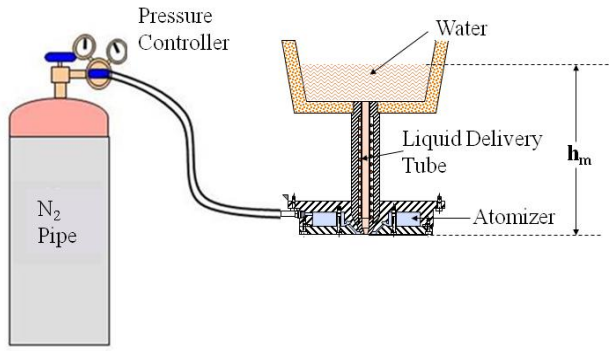


Figure 7. A sketch of the experimental assembly used for measuring $\dot{M}$.

4. RESULTS AND DISCUSSION

4.1 Measurement of aspiration pressure

A summary of the results is shown in Figure 8.

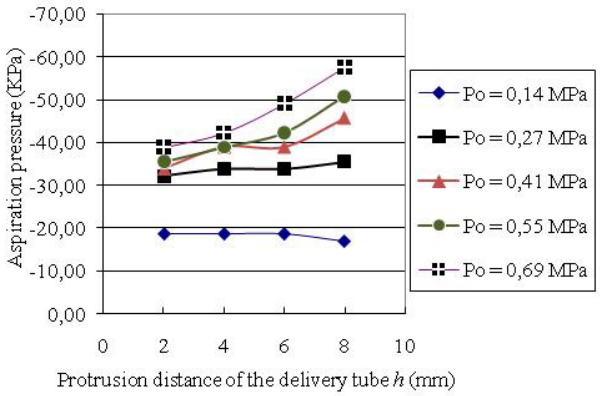


Figure 8. Aspiration pressure as a function of protrusion distance of the delivery tube *h* and atomization pressure P_o

It can be noted that in almost all of the atomization pressure range, the protrusion distance of the delivery tube *h* at which the maximum aspiration pressure is achieved is 8 mm. Moreover, the higher is *h*, the higher is the aspiration pressure, and the same behavior is seen in regard to P_o. In spite of that, no further tests were carried out with higher values for *h* because 8 mm is the geometrical limit of the design at which the gas leaves the nozzle without crashing onto the delivery tube, in order not to waste great quantities of kinetic energy of the gas.

A comparison with the literature [2, 4, 9] shows that the obtained results are quite higher for the same atomization pressure range, as a consequence of the ultrasonic gas flow and the higher gas mass flux rate $\dot{G}$, the latter because of the selection of a high total gas outlet area of the nozzle (as a result of the usage of an annular ring-shaped nozzle).

4.2 Measurements of gas mass flux rates $\dot{G}$

A summary of the obtained results is shown in It can be seen that there is a little difference between the results computed by means of the two different non-ideal gas equations used. However, due to Redlich-Kwong equation is more accurately for high pressures than Van der Waals equation, the former was taken as the reference to compare its results with the ones that were theoretically calculated. Accordingly, it can be noted that the average of the measurements is 81% that of the theoretically calculated values. This difference can be attributed to the following factors: first of all, no pressure lost

was taken into account, so gas pressure from the pipe to the exit of the nozzle was considered to be constant. Just the same, the presence of a "Vena Contracta" reduces apparently the gas mass flux rate, which is a main feature of an USGA [2] like the one that was designed in this work.

Table 3, for two different values of atomization pressure arbitrarily selected. Pipe and jet temperature at the exit of the atomizer were 298 K and 277 K, respectively.

It can be seen that there is a little difference between the results computed by means of the two different non-ideal gas equations used. However, due to Redlich-Kwong equation is more accurately for high pressures than Van der Waals equation, the former was taken as the reference to compare its results with the ones that were theoretically calculated. Accordingly, it can be noted that the average of the measurements is 81% that of the theoretically calculated values. This difference can be attributed to the following factors: first of all, no pressure lost was taken into account, so gas pressure from the pipe to the exit of the nozzle was considered to be constant. Just the same, the presence of a "Vena Contracta" reduces apparently the gas mass flux rate, which is a main feature of an USGA [2] like the one that was designed in this work.

Table 3. Determination of gas mass flux rates $\dot{G}$

Po (MPa) [1]	*T* (K)	$\dot{G}$ (Kg/min) [2]	$\dot{G}$ (Kg/min) [3]	$\dot{G}$ (Kg/min) [4]	% $\dot{G}$ Reduction [5]
0,8	298	2,183	1,635	1,709	74,91%
1,0	298	2,670	2,350	2,460	88,01%

[1] Manometric pressure

[2] Theoretically Calculated

[3] Experimentally Calculated by means of Redlich-Kwong equation

[4] Experimentally Calculated by means of Van der Waals equation

[5] Calculated regarding to Redlich-Kwong equation

A comparison with the literature [2, 4] shows that the measured values are pretty higher for the same atomization pressure range, which is desirable in order to obtain powders with lower mean mass diameter d_m, as it is predicted by equation (1). Nevertheless, it needs to be taken into account for the operation of the *Osprey* process, since it could lower the solidification time of the atomized powders, changing their morphology from spherical forms to flattened forms, and also increasing d_m if the second atomization stage is avoided. At the same time, the next steps of the *Osprey* process (injection and deposition) could be affected. If so, it would be pretty hard to exert a control on them [1].

4.3 Atomization water tests

From Figure 8, it can be noted that, for a same atomization pressure, the lowest aspiration pressure is almost always achieved with *h* being equal to 2 mm. On the other hand, 8 mm of protrusion distance of the delivery tube can almost always produce the highest values for aspiration pressure. Those limits were selected to be used in water atomization tests in order to determinate the effect of *h* on water mass flux rate $\dot{M}$. A summary of the obtained result can be seen in Figure 9.

It is clear that, when an atomization pressure exists, the water mass flux rate is higher than the one obtained as a result of a free-fall flow, which is only a consequence of the presence of an aspiration pressure at the end of the delivery tube.

Although the aspiration pressure is directly proportional to *h* accordingly to Figure 8, it can be noted from Figure 9 that the lowest value of *h* can achieve the highest values of $\dot{M}$. Moreover, $\dot{M}$ is directly proportional to P_o up until a certain value after which, $\dot{M}$ decreases with an increase of P_o.

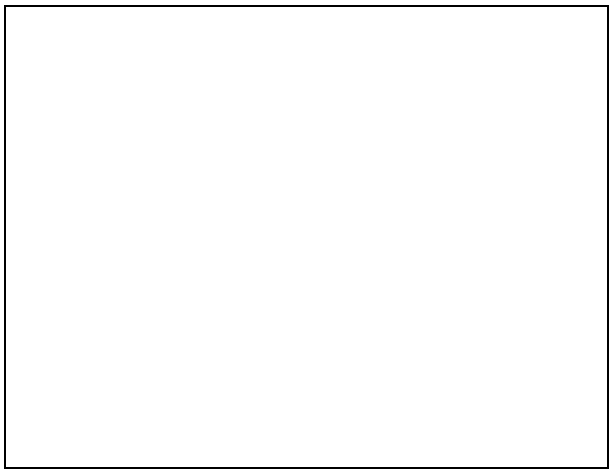


Figure 9. Water mass flux rate as a function of *h* and the atomization pressure.

The cause of this strange behavior is inside of the atomizer design. Because of the bottom of the atomizer was selected to be thick enough in order for it to withstand the demanding mechanical requirements, the nozzle and the end of the delivery tube are located inside of a "cone" (see Figure 10) which, in fact, acts as an extension of the confinement concept of the atomizer, enforcing the gas against the water flow as it comes out. Thus a force balance between the aspiration pressure and

the effect above described is established, which finally controls the water mass flux rate. That behavior is more marked for high pressures and protrusion distances.

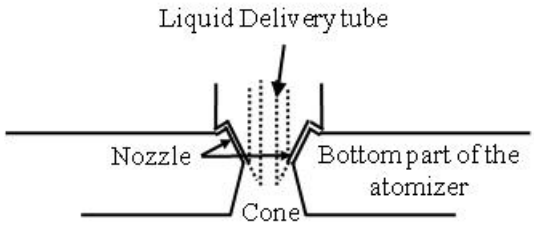


Figure 10. A sketch showing the location of the nozzle and the end of the delivery tube in the atomizer.

On the other hand, atomization test with wax were carried out. Wax was heated up to 393 K. The freeze-up effect was not observed in all cases.

4.4 Preliminary atomization test with aluminum

Finally, a preliminary atomization test with aluminum was carried out for an atomization pressure of 0,69 MPa. As a result, rounded powders within 40 and 80 µm diameter were obtained, as it can be noted from Figure 11.

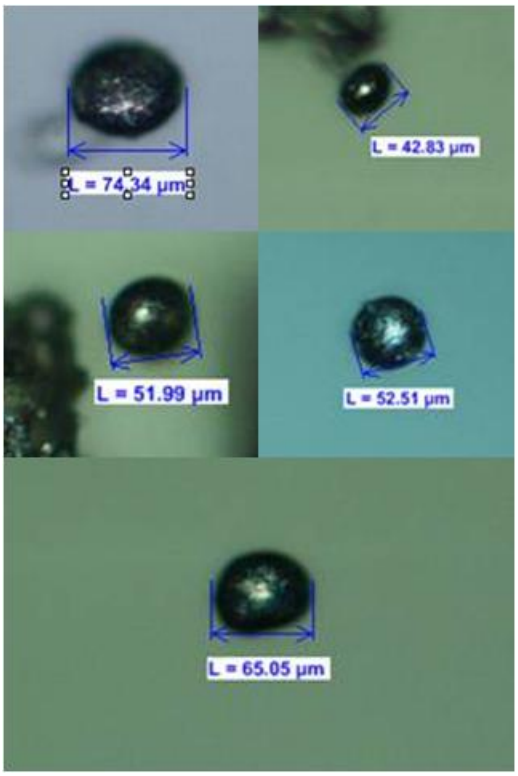


Figure 11. Pictures of some obtained powders, taken from an optic microscopy (500 X).

5. CONCLUSIONS

Observations and measurements have shown that the designed atomizer behaves as it was expected. But, due to the high gas mass flux rates obtained, it is very important to be careful when using the atomizer in the *Osprey* process, since it could produce desirable and non-desirable effects, depending on selected parameters of the process, such as metal superheat temperature and atomization pressure (i. e. heating the metal to a high enough temperature could avoid non-desirable effects, like flattened forms). Just the same, the better results were obtained if protrusion distance of the delivery tube was 8 mm, because it allowed getting a high aspiration pressure without wasting kinetic energy of the gas, and the liquid mass flux rates were not too high, which helps to get a low mean mass diameter in the powders, according to Lubanska's equation.

6. AKNOWLEDGMENTS

The authors would like to thank University of Valle, COLCIENCIAS, PTAR EMCALI and CARPAK S. A., for the help received during the development of this work.

7. REFERENCES:

[1] Atehortua D, Gonzalez J. "Diseño y construcción de un sistema Osprey para la producción de materiales compuestos de matriz de aluminio." Propuesta de tesis de pregrado para optar por el título de Ingeniero de Materiales. Universidad del Valle. 2008. p 164.

[2] Lavernia E. and Wu Y. "Spray Atomization and Deposition". John Wiley & Sons Ltda. (1996). Cap. 4

[3] Rivera O, Juárez H. "Atomización con Gas: Una Visión Actual". Depto. de Ingeniería Metalúrgica, Facultad de Química UNAM. Centro de Investigaciones en Materiales y Metalurgia, UAE. 2003.

[4] Nuñez I A, Lobel T, Palma R. "Atomizers for Molten Metals: Macroscopic Phenomena and Engineering Aspects". Atomization and Sprays, Vol 9, pp. 581-599, 1999.

[5] Garbero, M.; Vanni, M.; Fritsching, U. "Gas/surface heat transfer in spray deposition

processes". *International Journal of Heat and Fluid Flow.* Elsevier. 2005, p 18.

[6] Espina, P. I. "Study of an Underexpanded Annular Wall Jet Past an Axisymmetric Backward-Facing Step". Dissertation submitted to the Faculty of the Graduate School of the University of Maryland at College Park in partial fulfillment of the requirements for the degree of Doctor of Philosophy. University of Maryland. 1997. p 121.

[7] Sychev V, Vasserman A, Kozlov A, Spiridonov G. A., Tsymarny V. A.. "The Thermodynamic Properties of Nitrogen". Chapter 7. *Hemisphere Publishing Corporation, New York*. Energy Citations Database. 1987. p 297-368.

[8] Levy, Ariel. "Caracterización y diseño de atomizadores de flujos supersónicos para procesos pulvimetalúrgicos". Departamento de Ingeniería Mecánica. Facultad de Ciencias Físicas y Matemáticas. Universidad de Chile. 1997. p 39.

[9] Cui C, Cao F, Li Q. "Formation mechanism of the pressure zone at the tip of the melt delivery tube during the spray forming process". *Journal of Materials Processing Technology*. Elsevier. 2003. p 5.

[10] Castellan, G. W. "Fisicoquímica". *Fondo Educativo Interamericano*. 1976.